Accepted Manuscript

Title: Water-dispersible and quasi-superparamagnetic magnetite nanoparticles prepared in a weak basicity solution at the low synthetic temperature

Authors: Suhong Zhang, Kai Liu, Hangchao Chen, Shengyu Liu

PII: S0025-5408(17)34193-4
DOI: https://doi.org/10.1016/j.materresbull.2018.04.059
Reference: MRB 9997

To appear in: *MRB*

Received date: 9-11-2017
Revised date: 10-4-2018
Accepted date: 30-4-2018

Please cite this article as: Zhang S, Liu K, Chen H, Liu S, Water-dispersible and quasi-superparamagnetic magnetite nanoparticles prepared in a weak basicity solution at the low synthetic temperature, *Materials Research Bulletin* (2010), https://doi.org/10.1016/j.materresbull.2018.04.059

Water-dispersible and quasi-superparamagnetic magnetite nanoparticles prepared in a weak basicity solution at the low synthetic temperature

Suhong Zhang*[, a ,b, c], Kai Liu[a], Hangchao Chen[a], Shengyu Liu[a, b]

a. College of Mining Engineering, Taiyuan University of Technology, Taiyuan, 030024, China

b. Key Laboratory of In-situ Property-improving Mining of Ministry of Education, Taiyuan University of Technology, Taiyuan 030024, China

c. School of Chemical Engineering, University of Queensland, Brisbane, Queensland 4072, Australia

(**Corresponding Author. Tel.: +86 13453440746. E-mail address: zhangsh04@sina.com (Suhong Zhang)*)

Graphical abstract：

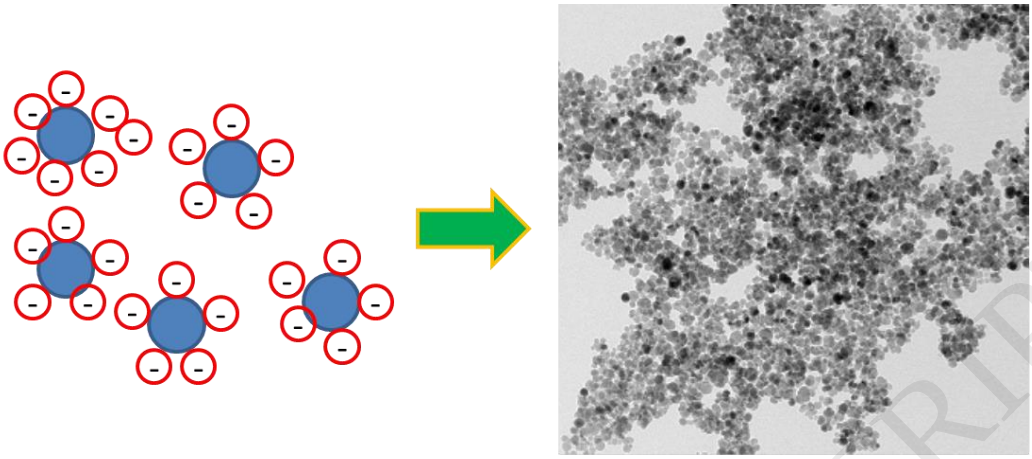

The good dispersion of magnetite nanoparticles in the aqueous solution was due to the coulomb repulsion that decreased the aggregation degree of magnetite particles. Thus, magnetite nanoparticles with a **quasi-**superparamagnetic property can be obtained by **the** co-precipitation method.

Highlights:

- Magnetite nanoparticles were prepared in a weak **basicity** solution at the low reaction temperature by **the** co-precipitation method.
- The double layer may be **steadily** formed on the **surfaces** of magnetite nanoparticles **when the pH value of the aqueous solution was over 9.**
- Magnetite nanoparticles present a **quasi-**superparamagnetic property and a good dispersion in the aqueous solution.

Abstract

Magnetite nanoparticles were prepared in a weak **basicity** solution at the low reaction temperature by **the** co-precipitation method. As a comparison, **the** oxidative precipitation method was also applied in this study. **The structure, morphology, and other properties** of the obtained samples were characterized by X-ray diffraction (XRD), Fourier transform infrared spectroscopy (FTIR), scanning electron microscope (SEM), transmission electron microscope (TEM), **and thermogravimetric analysis (TGA)**. The above characterization data indicate that small size and narrow size distribution are found for magnetite nanoparticles prepared by **the** co-precipitation method. Further magnetic property and Zeta potential results illuminate that magnetite nanoparticles prepared by this method **display** a **quasi-**superparamagnetic property and a good dispersion in the aqueous solution. Based on the investigation results, the magnetite nanoparticles with **a quasi-**superparamagnetic property and **a** fine dispersion can be facilely prepared in a weak **basicity** solution at the low reaction temperature by **the** co-precipitation method.

Key words: magnetite nanoparticles; superparamagnetic; co-precipitation; oxidative precipitation

1. Introduction

In recent few decades, magnetite (Fe_3O_4) nanoparticles have received extensive attention **due to their superparamagnetic property and potential applications compared with the bulk magnetite in bigger size** [1-**4**]. Magnetite nanoparticles

may be applied in the following fields, such as data storage materials, catalyst, ferrofluids and drug delivery [**5-7**]. Therefore, many reports on synthesis and characterization of magnetite nanoparticles were continuously published in the **papers** because of its great significance in various fields.

In view of potential applications of magnetite nanoparticles, the optimum magnetic property, morphology**,** and other physical properties were related to the synthesis methods. In the preparation process of magnetite nanoparticles, a few methods have been employed and recently developed, mainly consisting of co-precipitation **method**, sol-gel method, hydrothermal method**,** and electrochemical method [**8-15**]. Among these mentioned methods, co-precipitation method has been considered as a simple and convenient method for the synthesis of magnetite nanoparticles. But there is a problem that magnetite nanoparticles may be aggregated in the preparation process ascribed to the rapid crystallization speed of nanoparticles [**16**]. Furthermore, the aggregation of magnetic nanoparticles may also be related to their magnetic property. And thus **the particle size distribution** of the final product is broad.

In order to solve the above problems, various techniques such as ultrasonic, mechanochemical method and microwave have been applied in the co-precipitation process [**17-19**]. Meanwhile, various organic reagents such as polyvinylpyrrolidone, **cetyltrimethylammonium,** and oleic acid were added in order to avoid the aggregation of magnetite nanoparticles in the synthesis process **[20-22**]. And thus magnetic nanoparticles were encapsulated by organic reagents and had an enhanced

dispersibility. But some properties such as purity and saturation magnetization of magnetite nanoparticles were decreased after the addition of organic reagents. Therefore, it **was** very attractive that the dispersity of magnetic nanoparticles was increased **without using** organic **reagents** by the **co-precipitation** method in **the** practice.

In our present work, magnetite nanoparticles were successfully prepared in **a weak basicity solution** at low reaction temperature by **the** co-precipitation. As a comparison, the results of magnetite nanoparticles prepared by **the** oxidative precipitation were given in this study. The effects of preparation methods on structure, morphology and physical properties were discussed.

2. Experimental

2.1 Materials

In this study, ferrous chloride tetrahydrate ($FeCl_2 \cdot 4H_2O$), Ferric chloride hexahydrate ($FeCl_3 \cdot 6H_2O$), aqueous ammonia ($NH_3 \cdot H_2O$, 28%) and hydrogen peroxide (H_2O_2, 30%) were chemically pure and purchased from Tianjin Baishi Chemical Reagent Co. Ltd. **The distilled** water was used in the solution preparation process.

2.2 Preparation of magnetite nanoparticles

$FeCl_3 \bullet 6H_2O$ and $FeCl_2 \bullet 4H_2O$ were added **to** the distilled water by stirring of 500 rpm in nitrogen at room temperature and the molar ratio was 2:1. And then the solution temperature was increased to 60 °C via heating in the water bath and the aqueous solution of ammonia (1.5mol L^{-1}) was dropped as the water bath temperature

was 60 °C. The pH value of the solution was **adjusted between 9 and 10**. The solution was stirred at 60 °C for 3 h. At last, the precipitated magnetite was isolated by the magnet, washed several times with **the** distilled water and dried for 12 h at 60 °C in **a** vacuum oven. **Thus, the obtained sample was denoted as S_c. In addition, three repeated experiments were carried out and the product samples were denoted as S_{c1}, S_{c2}, S_{c3}, respectively.**

Oxidative precipitation method was also used in this study. $FeCl_2 \cdot 4H_2O$ were added **to** the distilled water by stirring of 500 rpm in nitrogen at room temperature. And then the solution temperature was increased to 60 °C and the aqueous solution of ammonia (1.5mol L^{-1}) was dropped as the water bath temperature reached 60 °C while the pH value of the solution was **adjusted in the range of 9 and 10**. Furthermore, the aqueous solution of hydrogen peroxide was also dropped via using the $FeCl_2 \cdot 4H_2O$ to H_2O_2 molar ratio of 3:1. The solution was vigorously stirred at 60 °C for 3 h. At last, the precipitated magnetite was separated by the magnet, washed several times with **the** distilled water and dried for 12 h at 60 °C in **a** vacuum oven. **Thus, the obtained sample was denoted as S_o.**

2.3 Characterization

Crystalline structures of magnetite nanoparticles were detected on an X-ray diffractometer (Bruker D_8 Advance, Germany) equipped with Cu-Kα radiation at 40 kV and 40 mA. Surface functional groups of the magnetite nanoparticles were obtained by a Fourier transform infrared spectroscopy (FTIR, Bruker, Tensor 27). Morphologies of magnetite nanoparticles were observed using a scanning electron

microscope (SEM, Zeiss, Merlin) and a transmission electron microscope images (TEM, JEOL, JEM-2010). Size **distributions** of nanoparticles were determined on a Mastersizer 3000. Magnetization **measurements of nanoparticles** were measured on a superconducting quantum interference device magnetometer at room temperature (SQUID, Quantum design MPMS3, USA). **The thermogravimetric analysis was performed on a NETZSCH STA 449 F3 from room temperature to 700 °C in a nitrogen atmosphere at a heating rate of 10 °C / min.** Zeta potentials of the samples were measured after the particles were dispersed in **the** distilled water **with** the pH value of 3 - 11. The zeta potential was obtained at least five measurements at the given pH value. Surface areas were measured at - 196 ℃ by using a Micromeritics ASAP 2020 gas adsorption analyzer.

3. Results and discussion

3.1 XRD analysis

XRD patterns of magnetite nanoparticles are **shown** in Fig.1. From this figure, it can be seen that the characteristic peaks of the obtained samples are sharp and obvious. The result indicates that a good crystallinity of the magnetite was gained in the preparation process. Seven characteristic peaks were observed at 2θ = 30.1°, 35.5°, 43.1°, 53.5°, 57.1°, 62.7° and 74.1° which were attributed to the (220), (311), (400), (422), (511), (440) and (533) indices of the magnetite, respectively [**23**]. The above **results are** consistent with the standard pattern in JCPD file (PDF No. 65-3107). The average **sizes** of magnetite nanoparticles **could** be calculated based on their XRD patterns according to Scherrer's formula and were given in Table 1.

Scherrer's formula, $D = k\lambda/\beta\cos\theta$, where D is particle sizes, k is a constant 0.9, λ is X-ray wavelength (0.15406 nm), θ is diffraction angle, β is full-width at half-maximum of the diffraction line [**24**]. It is **concluded** that the **particle** size by co-precipitation method is less than that by oxidative precipitation method (Table 1), which may result in that XRD characteristic peaks of magnetite nanoparticles by **the** co-precipitation method are relatively broader than that by **the** oxidative precipitation method **(Fig. 1)**. **In order to illustrate the reproducibility of magnetite nanoparticles by the co-precipitation method, three repeated experiments were carried out.** XRD **patterns of the obtained samples were shown in Fig. 1. Three particle sizes were 12.6 nm (S_{c1}), 11.4 nm (S_{c2}) and 15.3nm (S_{c3}) calculated from Scherrer formula, respectively. The above results indicate that the similar magnetite nanoparticles can be repeatedly prepared by the co-precipitation method.**

3.2 FTIR analysis

The FT-IR spectra of magnetite nanoparticles are shown in Fig. 2. The strong characteristic **peaks** of Fe-O functional group appeared at around 575 cm^{-1} indicating the formation of magnetite nanoparticles [**25**]. The characteristic peak of the bulk magnetite was 570 cm^{-1} [**26, 27**]. Compared to that of the bulk magnetite, the FTIR **spectra** of magnetite nanoparticles presented a blue shift and the characteristic **peaks** of magnetite nanoparticles **were** at around 575 cm^{-1}. Two characteristic peaks were found at 3421cm^{-1} and 1628 cm^{-1} attributed to the stretching vibration of O-H bond and the bending vibration of O-H bond, respectively [**28, 29**]. The presence of O-H

bond may be related to OH groups on magnetite nanoparticles and **water molecules adsorbed on the surfaces** of magnetite nanoparticles. In addition, compared Fig. 2a with Fig. 2b, two characteristic peaks of O-H bond in magnetite nanoparticles by **the** co-precipitation method were higher than those in magnetite nanoparticles by **the** oxidative precipitation method. The result may be due to the fact that the surface area of magnetite nanoparticles by **the** co-precipitation method (80.4 m^2 / g) was **larger** than that of magnetite nanoparticles by **the** oxidative precipitation method (49.3 m^2 / g) (Table 1). Nanoparticles can exhibit **high** surface-to-volume atomic ratio, high surface activity, and amount of dangling bonds on the surface. The larger **the surface area** is, the more OH groups are formed and the more molecules are adsorbed.

3.3 Structure and morphology

The morphologies of magnetite nanoparticles are shown in Fig. 3. From Fig. 3a and Fig. 3b, it can be observed that magnetite nanoparticles prepared by **the** co-precipitation method are all sphere-like structures while those prepared by **the** oxidative precipitation method are oval-shaped structures. In Fig. 3a and Fig. 3b, it can be found that magnetite nanoparticles prepared by **the** oxidative precipitation method are relatively seriously aggregated. In order to observe and determine the accurate sizes of magnetite nanoparticles, TEM images of magnetite nanoparticles were investigated as presented in Fig. 3. From Fig. 3c and Fig. 3d, the **average** sizes of nanoparticles were around 14.4 nm and 28.6 nm, respectively. As shown in Table 1, the **average** sizes of nanoparticles based on TEM were well coincident with those calculated from XRD patterns according to Scherrer's formula [**30**].

The size distributions were recorded by measuring the particle sizes of the obtained samples and the histograms have been shown in Fig. 4. For co-precipitation method (Fig. 4a), the size of particles is changed from 10.9 to 26.4 nm and the **average** size is 15.3 ± 0.3 nm. For oxidative precipitation method (Fig. 4b), a fairly large size varies in the range of 19.7 to 85.5 nm and the **average** size is up to 30.4 ± 0.9 nm. From Table 1, it can be seen that the particle **sizes** measured by **the** size distribution technique **were** slightly larger than those determined by XRD and TEM and may be larger than the real **sizes** [**31**]. In addition, from Fig. 4, it can be found that the size distribution of particles via **the** co-precipitation method is relatively narrow and the particle **sizes are** also small based on the above results.

3.4 Magnetic property

The magnetic properties of magnetite nanoparticles were investigated and the magnetization curves were shown in Fig. 5. From Fig. 5a, the saturation magnetization value of magnetite nanoparticles was 67.8 emu/g when the external magnetic field was increased up to 20,000 Oe. At the same time, it can be found that there was a very slight hysteresis in the hysteresis loop and the values of **the** coercive field (H_c) **and the** remanent magnetization (M_r) were 9.5 Oe and 1.8 eum/g (Fig. 5a, red inset and Table 1), **respectively**. **Therefore, it is** concluded that magnetite nanoparticles prepared by **the** co-precipitation method present a **quasi-**superparamagnetic property [**32-34**]. From Fig.5b, the saturation magnetization value of magnetite nanoparticles was 73.2 emu/g when the external magnetic field was increased up to 20,000 Oe. But, there was an obvious hysteresis in the hysteresis loop

and the values of **the** coercive field (H_c) and **the** remanent magnetization (M_r) were 73.6 Oe and 11.8 eum/g (Fig. 5b, blue inset and Table 1), respectively. Magnetite nanoparticles present a superparamagnetism when the particle size is less than about 30 nm [**23**]. Based on the size distribution results, **the sizes of particles are in the range of 10.9 to 26.4 nm for the co-precipitation method and 19.7 to 85.5 nm for the oxidative precipitation method, respectively.** When magnetite nanoparticles were prepared by **the** oxidative precipitation method, there **was** a certain part of particles beyond 30 nm, and thus an obvious hysteresis in the hysteresis loop **was** given. In addition, the saturation magnetization values of magnetite nanoparticles via two above synthesis **methods** are less than the saturation magnetization value of **the** bulk magnetite [**35**]. This phenomenon may be due to the smaller size of magnetite nanoparticles and their surface disorder. When the size of the nanoparticles decreased, the surface of the nanoparticles increased as mentioned in Table 1. And thus more canted or disordered spins were presented, which resulted in the increase of the surface spins disorientation. At last, the saturation magnetization value decreased [**36**].

3.5 Thermogravimetric analysis

Two weight changes of magnetite nanoparticles with the increase of the heating temperature were investigated by thermogravimetric analysis as shown in Fig. 6. Curve (a) shows that the first weight loss from room temperature to 150 °C was about 0.5%, which was due to physically adsorbed water molecules on the surfaces of magnetite particles [**37**]**. The further weight loss between**

150 °C and 370 °C was about 1.3%, which was assigned to chemisorbed water molecules and the dehydroxylation of magnetite particles [**38, 39**]**. When the heating temperature increased up to 700 °C, the final weight loss was about 1.3%, which may be ascribed to the phase transition of magnetite to iron (II) oxide because of the stable phase of iron (II) oxide at higher temperatures** [**40**]**. Curve (b) shows a similar variation to curve (a). However, the total weight loss of the curve (a) was more than that of the curve (b), which was due to the properties of magnetite particles (S_c) including small particle size, large surface area and abundant hydroxyls based on the characterization results of XRD, FTIR and surface area. In addition, the total weight losses were about 3.1% (S_c) and 2.3% (S_o) between room temperature and 700 °C, respectively, indicating both samples displayed a favorable thermal stability.**

3.6 Zeta Potential measurement

The zeta potential was measured as a function of pH for magnetite particles prepared by **the** co-precipitation method as shown in Fig. 7. From this figure, it can be seen that the isoelectric point of magnetite particles is in the pH range of 3 to 4 and decreased compared to the published **papers** [**12, 41, 42]** due to a large number of OH groups on its surface according to the FTIR result. The phenomenon indicates that the magnetite particles may be stably suspended in the aqueous solution with a broader pH value. With the increase of pH value, the zeta potential value of magnetite particles constantly decreased. When the pH value was over 9, the zeta potential value was about - 31 mV. Magnetic metal oxide particles in the aqueous solution **are** usually

in the form of M-OH ((M, metal atom; OH, hydroxyl). As shown in **Scheme** 1, when the pH value of the aqueous solution increased M-OH tended to release $\mathbf{H^+}$ resulting in the transformation of MO^-. Thus the double layers formed on the **surfaces** of the metal oxide particles. The aggregation degree of magnetite particles was decreased due to the **Coulomb** repulsion, which contributed to the good dispersion of magnetite nanoparticles in the aqueous solution [**43**]. Therefore, magnetite nanoparticles in the aqueous solution with a good dispersion were obtained and showed a **quasi-**superparamagnetic property **by the** co-precipitation method.

4. Conclusions

Magnetite nanoparticles were prepared by **the** co-precipitation method and **the** oxidative precipitation method in a weak **basicity** solution at **the** low reaction temperature. XRD results indicate that magnetite nanoparticles have been prepared by two methods. **Thermogravimetric analysis indicates both samples display a favorable thermal stability.** According to FT-IR spectra, the amount of OH groups on the surface area of magnetite nanoparticles by **the** co-precipitation method was more than that of OH groups on the surface area of magnetite nanoparticles by **the** oxidative precipitation method. TEM and size distribution results illuminate that a fairly narrow size of **magnetite** nanoparticles was obtained by **the** co-precipitation method. Magnetization measurement **confirms** a **quasi-**superparamagnetic property and zeta potential measurement **shows** a good dispersion of magnetite nanoparticles in the aqueous solution. Therefore, **the** water-dispersible and **quasi-**superparamagnetic magnetite nanoparticles can be prepared by **the**

co-precipitation method.

Acknowledgements

The author thanks for the financial support of the National Natural Science Foundation of China (No.51304144), the Study Abroad Program for the University-Sponsored Young Teachers (2017, Taiyuan University of Technology), Qualified Personnel Foundation of Taiyuan University of Technology (No.tyutrc-201222a), Research Project Supported by Shanxi Scholarship Council of China (No. 2011-039) and Fund Program for the Scientific Activities of Selected Returned Overseas Professionals in Shanxi Province (No. 2011-762).

Referencens

[1] Y. Min, M. Akbulut, K. Kristiansen, Y. Golan, J. Israelachvili, The role of interparticle and external forces in nanoparticle assembly, Nat. Mater. 7 (2008), 527-538.

[2] P. Wang, C. Lee, T. Young, D. Lin, W. Chiu, Preparation and clinical application of immunomagnetic latex, J. Polym. Sci. Part A: Polym. Chem. 43 (2005) 1342 - 1356.

[3] J. P. Cheng, X. B. Zhang, G. F. Yi, Y. Ye, M. S. Xia, Preparation and magnetic properties of iron oxide and carbide nanoparticles in carbon nanotube matrix, J. Alloy. Compd. 455 (2008) 5 - 9.

[4] W. Wu, Z. H. Wu, T. Yu, C. Z. Jiang, W. Kim, Recent progress on magnetic iron oxide nanoparticles: synthesis, surface functional strategies and biomedical applications, Sci. Technol. Adv. Mat. 16 (2015) 023501(43pp).

[5] S. X. Zhang, X. L Zhao, H.Y. Niu, Y. L.Shi, Y. Q. Cai, G. B. Jiang,

Superparamagnetic Fe3O4 nanoparticles as catalysts for the catalytic oxidation of phenolic and aniline compounds, J. Hazard. Mater. 167 (2009) 560 - 566.

[6] A. S. Teja, P. Y. Koh, Synthesis, properties, and applications of magnetic iron oxide nanoparticles, Prog. Cryst. Growth Ch. 55 (2009) 22 - 45.

[7] S. Laurent, D. Forge, M. Port, A. Roch, C. Robic, L.Vander Elst, R. N. Muller, Magnetic iron oxide nanoparticles: synthesis, stabilization, vectorization, physicochemical characterizations, and biological applications, Chem. Rev. 108 (2008) 2064 - 2110.

[8] V. P. Ponomar, Synthesis and magnetic properties of magnetite prepared by chemical reduction from hematite of various particle sizes, J. Alloy. Compd. 741 (2018) 28 - 34.

[9] L. B. Tahar, M. H. Oueslati, M. J. A. Abualreish, Synthesis of magnetite derivatives nanoparticles and their application for the removal of chromium (VI) from aqueous solutions, J. Colloid. Interf. Sci. 512 (2018) 115 - 126.

[**10**] N. Asim, Synthesis of Fe_3O_4 nanocrystals using hydrothermal approach, J. Magn. Magn. Mate. 324 (2012) 4147 - 4150.

[**11**] K. Raja, S. Verma, S. Karmakar, S. Kar, S. Jerome Das, K. S. Bartwal, Synthesis and characterization of magnetite nanocrystals, Cryst. Res. Technol. 46 (2011) 497 - 500.

[12] J. J. Liu, C. Dai, Y. D. Hu, Aqueous aggregation behavior of citric acid coated magnetite nanoparticles: Effects of pH, cations, anions, and humic acid, Environ. Res. 161, (2018) 49 - 60.

[13] M. K. Poddar, M. Arjmand, U. Sundararaj, V. S. Moholkar, Ultrasound-assisted synthesis and characterization of magnetite nanoparticles and poly(methyl methacrylate)/magnetite nanocomposites, Ultrason. Sonochem. 43 (2018) 38 - 51.

[14] S. M. Vidojkovic, M. P. Rakin, Surface properties of magnetite in high temperature aqueous electrolyte solutions: A review, Adv. Colloid Interfac. 245 (2017) 108 - 129.

[15] A. Bahadur, A. Saeed, M. Shoaib, S. Iqbal, M. I. Bashir, M. Waqas, M. Nasir Hussain, N. Abbas, Eco-friendly synthesis of magnetite (Fe_3O_4) nanoparticles with tunable size: Dielectric, magnetic, thermal and optical studies, Mater. Chem. Phys. 198 (2017) 229 - 235.

[**16**] K. Tao, H. Dou, K. Sun, Interfacial coprecipitation to prepare magnetite nanoparticles: concentration and temperature dependence, Colloids Surface A 320 (2008) 15 - 122.

[**17**] N. Wang, L. H. Zhu, D. L. Wang, M. Q. Wang, Z. F. Lin, H. Q. Tang, Sono-assisted preparation of highly-efficient peroxidase-like Fe_3O_4 magnetic nanoparticles for catalytic removal of organic pollutants with H_2O_2, Ultrason. Sonochem. 17 (2010) 526 - 533.

[**18**] T. Iwasaki, K. Kosaka, T. Yabuuchi, S. Watano, T. Yanagida, T. Kawai, Novel mechanochemical process for synthesis of magnetite nanoparticles using coprecipitation method, Adv. Powder Technol. 20 (2009) 521 - 528.

[**19**] R. Y. Hong, T. T. Pan, H. Z. Li, Microwave synthesis of magnetic Fe_3O_4

nanoparticles used as a precursor of nanocomposites and ferrofluids, J. Magn. Magn. Mater. 303 (2006) 60 - 68.

[**20**] R. L. D. Loyo, S. I. Nikitenko, A. C. Scheinost, M. Simonoff, Immobilization of selenite on Fe_3O_4 and Fe/Fe_3C ultrasmall particles, Environ. Sci. Technol. 42 (2008) 2451 - 2456.

[**21**] S. Bolisetty, J. J. Vallooran, J. Adamcik, R. Mezzenga, Magnetic-responsive hybrids of Fe_3O_4 nanoparticles with β-lactoglobulin amyloid fibrils and nanoclusters, ACS Nano 7 (2013) 6146 - 6155.

[**22**] Pei Li, Ai Mei Zhu, Qing Lin Liu, Qiu Gen Zhang, Fe_3O_4/poly (N-Isopropylacrylamide)/chitosan composite microspheres with multiresponsive properties, Ind. Eng. Chem. Res. 47(2008) 7700 - 7706.

[**23**] Y. X. Dong, B. Wen, Y. J. Chen, P. Q. Cao, C. C. Zhang, Autoclave-free facile approach to the synthesis of highly tunable nanocrystal clusters for magnetic responsive photonic crystals, RSC Adv. 6 (2016) 64434 - 64440.

[**24**] Y. Deng, L.Wang, W.Yang, S. Fu, A. Elaissari, Preparation of magnetic polymeric particles via inverse microemulsion polymerization process, J. Magn. Magn. Mater. 257 (2003) 69 - 78.

[**25**] C. A. Dincer, Y. Nuray, A. Nihal, C. Ayla, A comparative study of Fe_3O_4 nanoparticles modified with different silane compounds, Appl. Surf. Sci. 318 (2014) 297 - 304.

[**26**] M. Ma, Y. Zhang, W. Yu, H. Y. Shen, H. Q. Zhang, N. Gu, Preparation and characterization of magnetite nanoparticles coated by amino silane, Colloids Surfaces

A 212 (2003) 219 - 226.

[**27**] C. C. Lina, J. M. Ho, Structural analysis and catalytic activity of Fe_3O_4 nanoparticles prepared by a facile co-precipitation method in a rotating packed bed, Ceram. Int. 40 (2014) 10275 - 10282.

[**28**] L. G. Bach, M. R. Islam, J. T. Kim, S.Y. Seo, K. T. Lim, Encapsulation of Fe_3O_4 magnetic nanoparticles with poly (methyl methacrylate) via surface functionalized thiol-lactam initiated radical polymerization, Appl. Surf. Sci. 258 (2012) 2959 - 2966.

[**29**] J. M. Qu, G. Liu, Y. M. Wang, R. Y. Hong, Preparation of Fe_3O_4 - chitosan nanoparticles used for hyperthermia, Adv. Powder Technol. 21 (2010) 461- 467.

[**30**] Jun Hu, Xijian Hu, Aimin Chen, Shaofen Zhao, Directly aqueous synthesis of well-dispersed superparamagnetic Fe3O4 nanoparticles using ionic liquid-assisted co-precipitation method, Journal of Alloys and Compounds 603 (2014) 1–6

[**31**] M. R. Ghazanfari, M. Kashefi, M. R. Jaafari, Optimizing and modeling of effective parameters on the structural and magnetic properties of Fe_3O_4 nanoparticles synthesized by coprecipitation technique using response surface methodology, J. Magn. Magn. Mater. 409 (2016) 134 - 142.

[**32**] P. Li, A. Zhu, Q. Liu, Q. Zhang, Fe_3O_4/poly (N-Isopropylacrylamide) - /-chitosan composite microspheres with multiresponsive properties, Ind. Eng. Chem. Res. 47 (2008), 7700 - 7706.

[**33**] Q. L. Hu, F. P. Chen, B. Q. Li, J. C. Shen, Preparation of three dimensional nano-magnetite/chitosan rod. Mater. Lett. 60 (2006) 368 - 370.

[**34**] R.Y. Hong, B .Feng, G. Liu, S. Wang, H. Z. Li, J. M. Ding, Y. Zheng, D. G. Wei,

Preparation and characterization of Fe_3O_4/polystyrene composite particles via inverse emulsion polymerization, J. Alloy. Compd. 476 (2009) 612 - 618.

[**35**] M. Yamaura, R. L. Camilo, L. C. Sampaio, M. A. Macêdo, M. Nakamura, H. E. Toma, Preparation and characterization of (3-aminopropyl) triethoxysilane-coated magnetite nanoparticles, J. Magn. Magn. Mater. 279 (2004) 210 - 217.

[**36**] K. Maaz, S. Karim, A. Mumtaz, S. K. Hasanain, J. Liu, J. L. Duan, Synthesis and magnetic characterization of nickel ferrite nanoparticles prepared by co-precipitation route, J. Magn. Magn. Mater. 321(2009) 1838 - 1842.

[37] F. Askari, E. Ghasemi, B. Ramezanzadeh, M. Mahdavian, Synthesis and characterization of the fourth generation of zinc phosphate pigment in the presence of benzotriazole, Dyes Pigments 124 (2016) 18 - 26.

[38] M. Izadi, T. Shahrabi, B. Ramezanzadeh, Synthesis and characterization of an advanced layer-by-layer assembled Fe_3O_4/polyaniline nanoreservoir filled with Nettle extract as a green corrosion protective system, J. Ind. Eng. Chem. 57 (2018) 263 - 274.

[39] B.A. Bhanvase, M. A. Patel, S.H. Sonawane, Kinetic properties of layer-by-layer assembled cerium zinc molybdate nanocontainers during corrosion inhibition, Corros. Sci. 88 (2014) 170 - 177.

[40] S.Y. Zhao, D. K. Lee, C. W. Kim, H. G. Cha, Y. H. Kim, Y. S. Kang, Synthesis of magnetic nanoparticles of Fe_3O_4 and $CoFe_2O_4$ and their surface modification by surfactant adsorption, Bull. Korean Chem. Soc. 27 (2006) 237 - 242.

[**41**] S. Bhattacharya, F. Eckert, V. Boyko, A. Pich, Temperature-, pH-, and magnetic-field-sensitive hybrid microgels, Small 3 (2007) 650 - 657.

[42] Y. Qiu, H. Guo, C. F. Guo, J. Z. Zheng, T. L. Yue, Y. H. Yuan, One-step preparation of nano-Fe_3O_4 modified inactivated yeast for the adsorption of patulin, Food Control 86 (2018) 310 - 318.

[**43**] R. H. Kodama, A. E. Berkowetz, E. J. Mcnifr,, Surface spin disorder in $NiFe_2O_4$ nanoparticIes, Phys. Rev. Lett. 77 (1996) 394 - 397.

Captions for figures and tables:

Fig. 1. XRD patterns of magnetite nanoparticles: (a) co-precipitation method; (b) oxidative precipitation method.

Fig. 2. FT-IR spectra of magnetite nanoparticles prepared by (a) co-precipitation method; (b) oxidative precipitation method.

Figure 3. SEM and TEM images of magnetite nanoparticles: (a), (c) co-precipitation method; (b), (d) oxidative precipitation method; (scale bars in figures are 100 nm).

Fig. 4. Size distributions of magnetite nanoparticles: (a) co-precipitation method; (b) oxidative precipitation method.

Fig. 5. Field dependent magnetization curves for magnetite nanoparticles prepared by (a) co-precipitation method, red inset is the magnification of the magnetization curve in the mangnetic field from -100 Oe to 100 Oe; (b) oxidative precipitation method, blue inset is the magnification of the magnetization curve in the mangnetic field from -200 Oe to 200 Oe.

Fig. 6. Thermogravimetric analysis curves: (a) co-precipitation method; (b) oxidative precipitation method.

Fig.7. Zeta potentials of magnetite nanoparticles prepared by co-precipitation method. Five measurements were at least conducted for each condition, and the error bars represented the standard deviations.

Table 1. List of particle sizes, Mr, Hc, and surface areas of the samples.

Scheme 1. The dispersion process of magnetite nanoparticles in the aqueous solution.

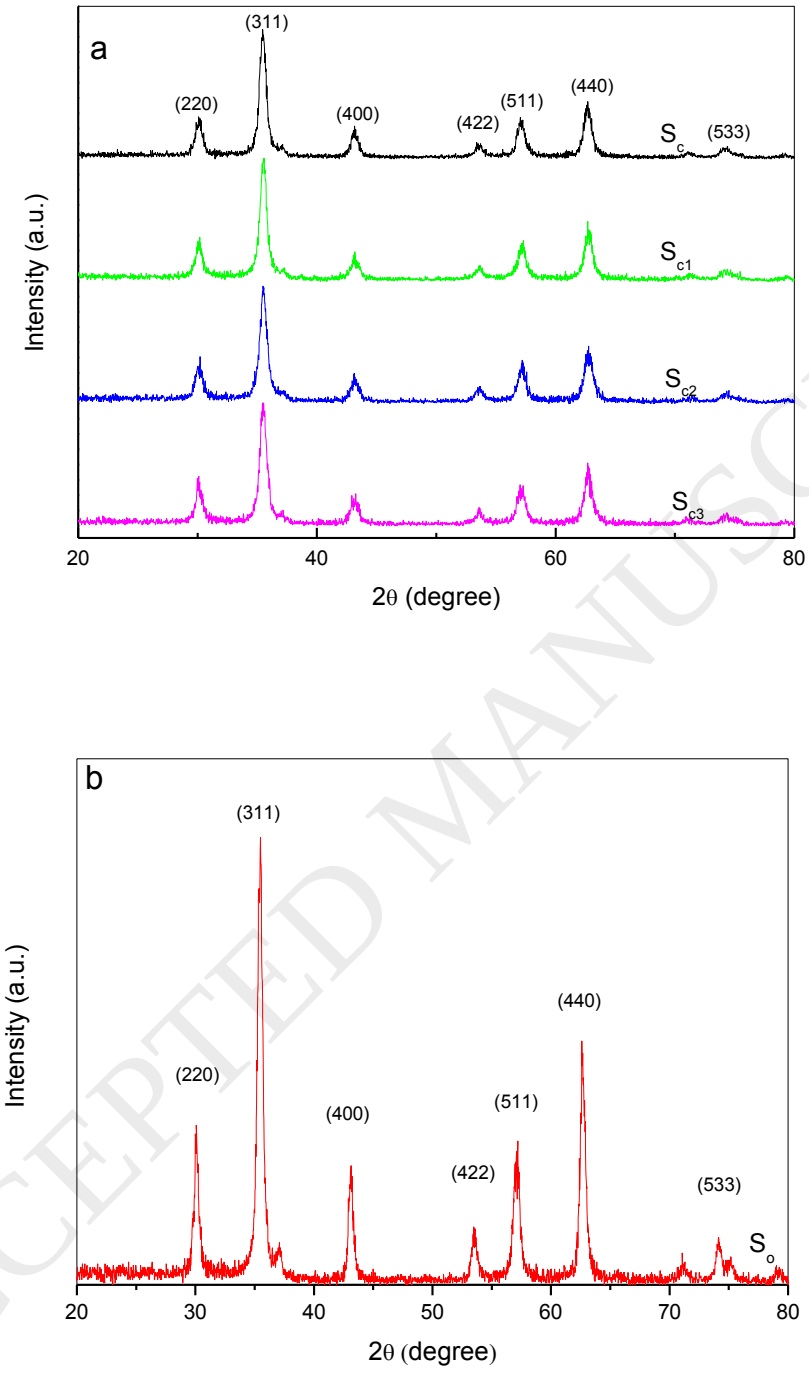

Fig. 1. XRD patterns of magnetite nanoparticles: (a) co-precipitation method; (b) oxidative precipitation method.

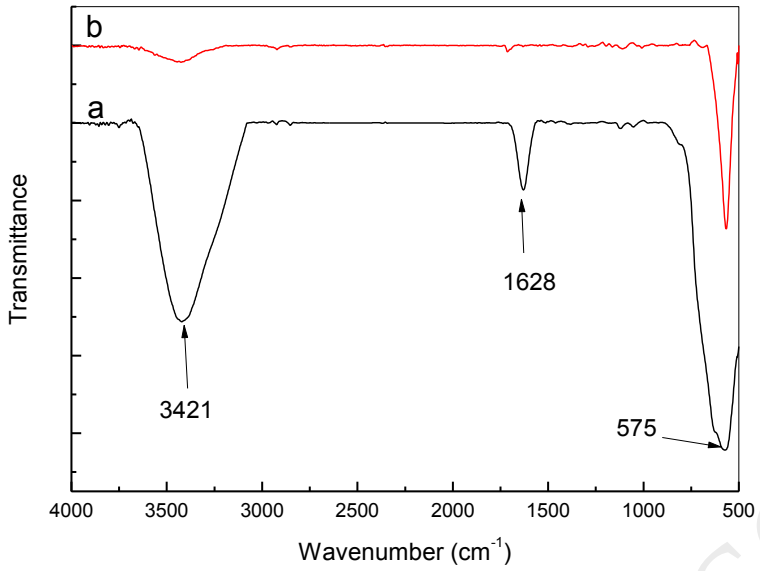

Fig. 2. FT-IR spectra of magnetite nanoparticles prepared by (a) co-precipitation method; (b) oxidative precipitation method.

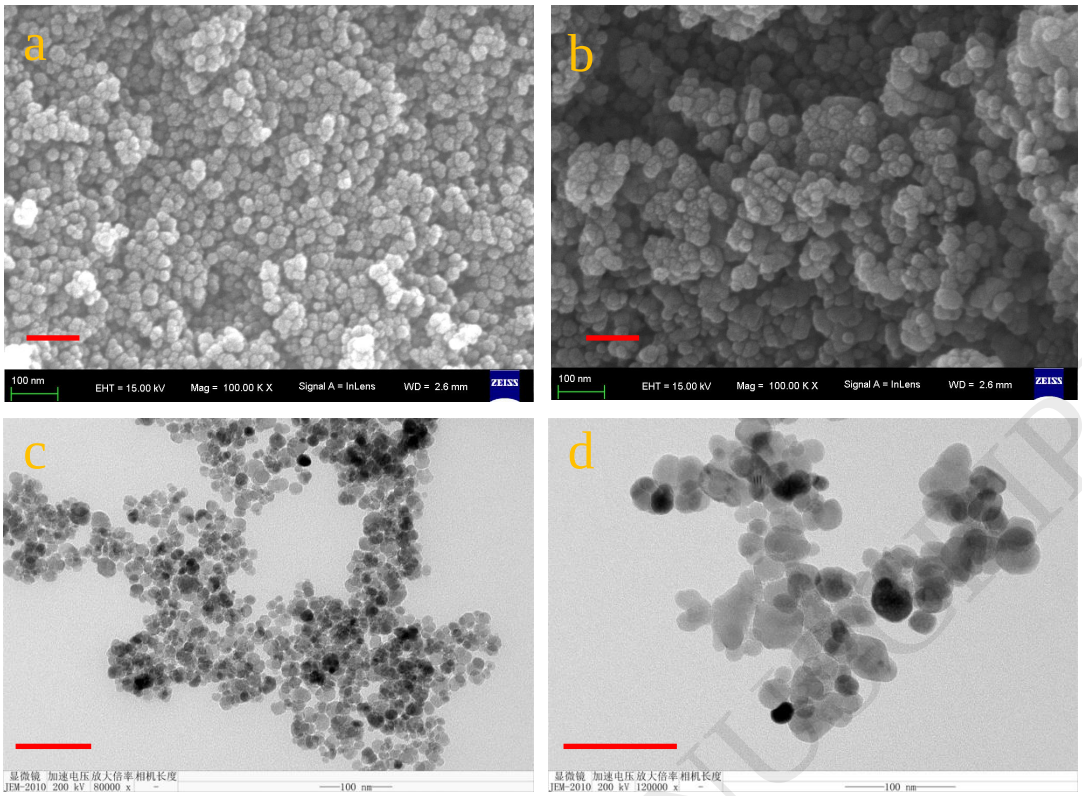

Fig. 3. SEM and TEM images of magnetite nanoparticles: (a), (c) co-precipitation method; (b), (d) oxidative precipitation method; (scale bars in figures are 100 nm).

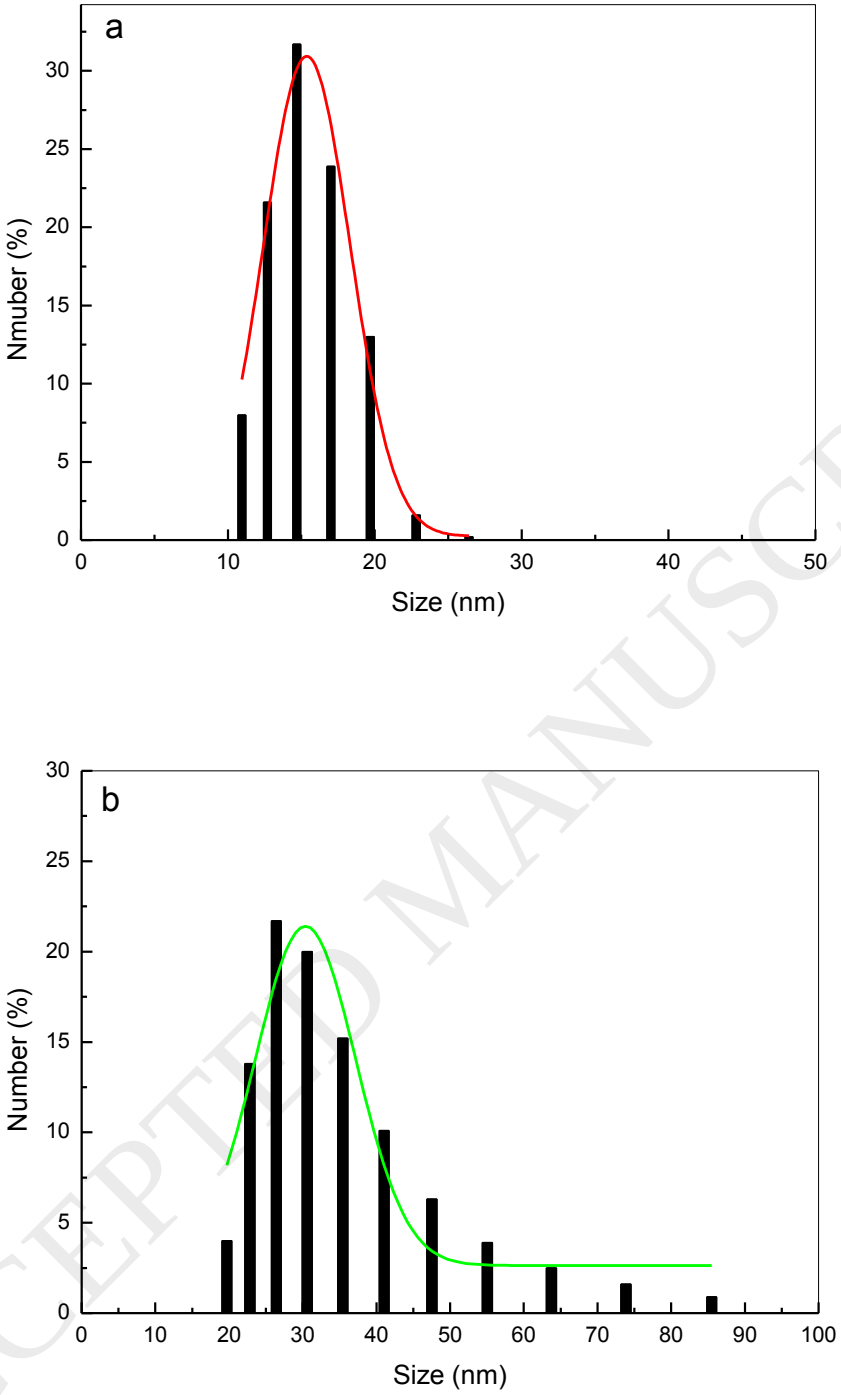

Fig. 4. Size distributions of magnetite nanoparticles: (a) co-precipitation method; (b) oxidative precipitation method.

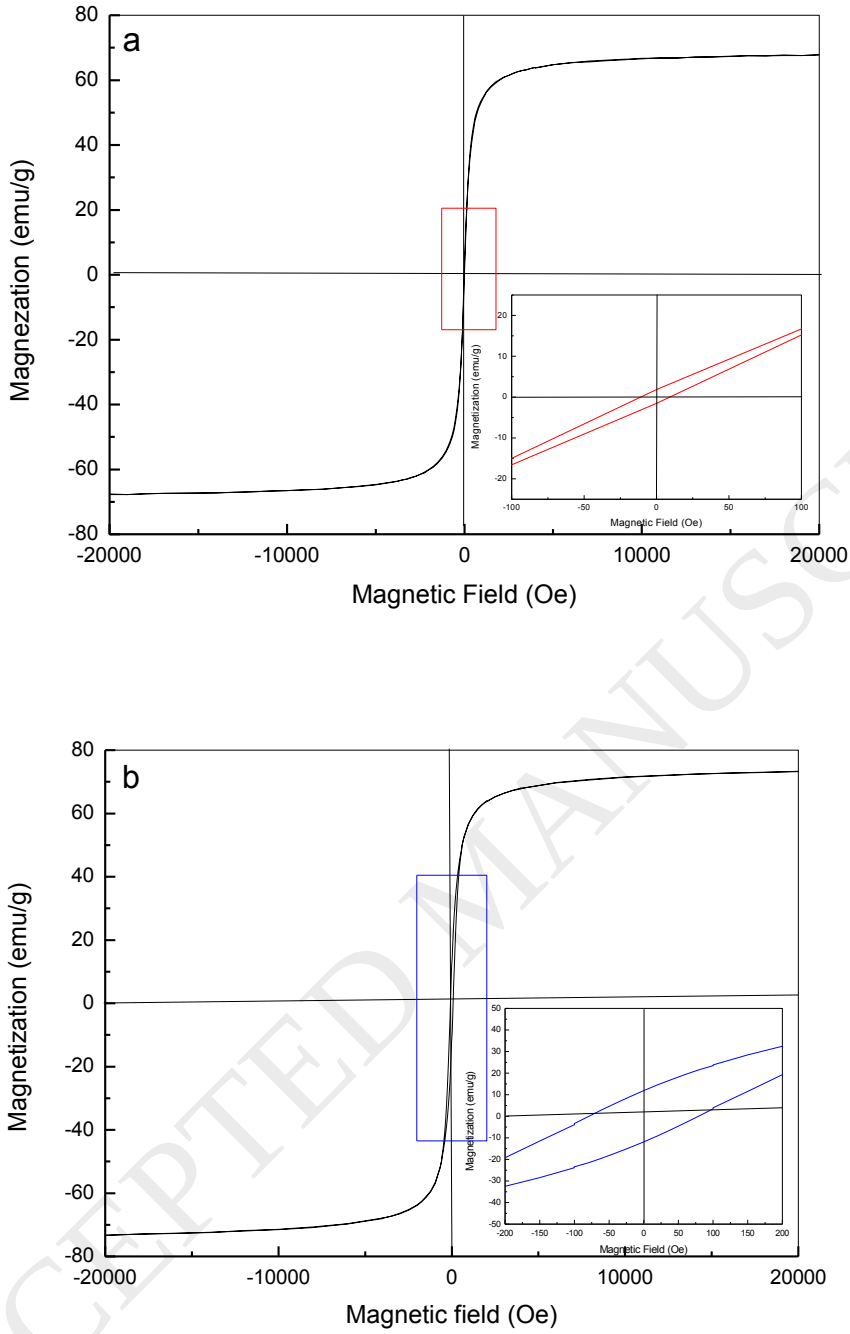

Fig. 5. Field dependent magnetization curves for magnetite nanoparticles prepared by (a) co-precipitation method, red inset is the magnification of the magnetization curve in the mangnetic field from -100 Oe to 100 Oe; (b) oxidative precipitation method, blue inset is the magnification of the magnetization curve in the mangnetic field from -200 Oe to 200 Oe.

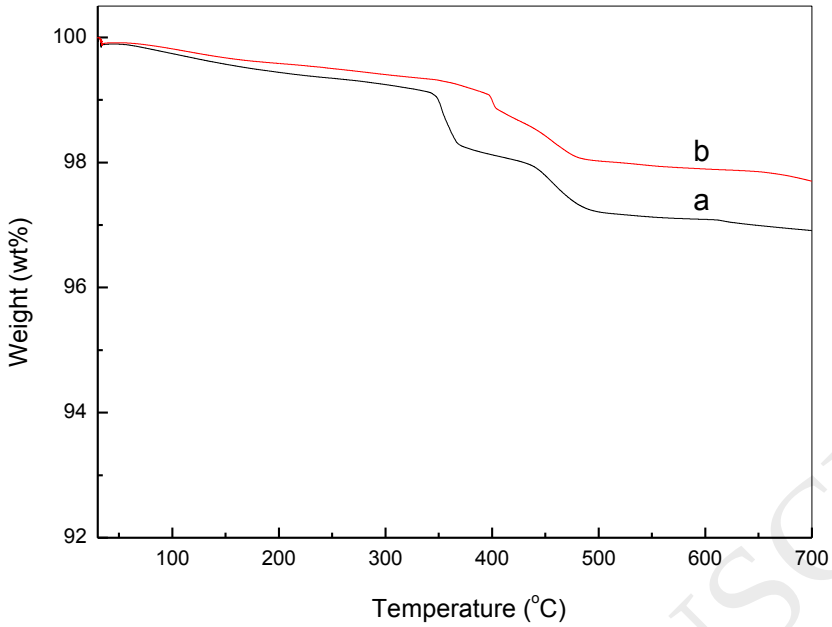

Fig. 6. Thermogravimetric analysis curves: (a) co-precipitation method; (b) oxidative precipitation method.

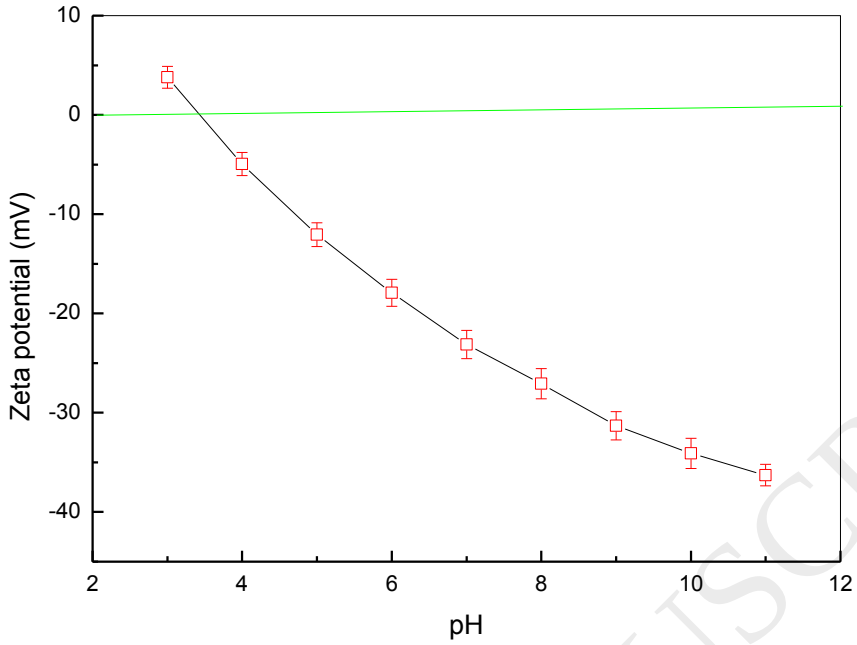

Fig. 7. Zeta potentials of magnetite nanoparticles prepared by co-precipitation method. **Five measurements were at least conducted for each condition, and the error bars represented the standard deviations.**

Table 1. List of particle sizes, M_r, H_c, and surface areas of the samples.

Magnetite	d_{XRD} (nm)	D_{TEM} (nm)	D [c] (nm)	M_r (emu.g^{-1})	H_c (Oe)	surface area (m^2/g)
S_c[a]	13.6	14.4	15.3 ± 0.3	1.8	9.5	80.4
S_o[b]	27.4	28.6	30.4 ± 0.9	11.8	73.6	49.3

[a.] co-precipitation method; [b.] oxidative precipitation method; c. determined by a Mastersizer 3000

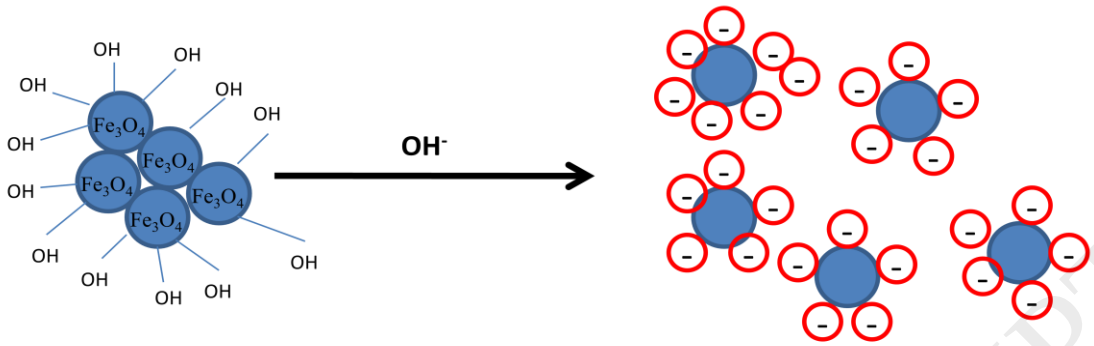

Scheme 1. The dispersion process of magnetite nanoparticles in the aqueous solution.